Article

Generation of Oxide Nanopatterns by Combining Self-Assembly of S-Layer Proteins and Area-Selective Atomic Layer Deposition

Jiurong Liu, Yuanbing Mao, Esther Lan, Diosdado Rey Banatao, G. Jason Forse, Jun Lu, Hans-Olof Blom, Todd O. Yeates, Bruce Dunn, and Jane P. Chang

J. Am. Chem. Soc., **2008**, 130 (50), 16908-16913 • DOI: 10.1021/ja803186e • Publication Date (Web): 19 November 2008

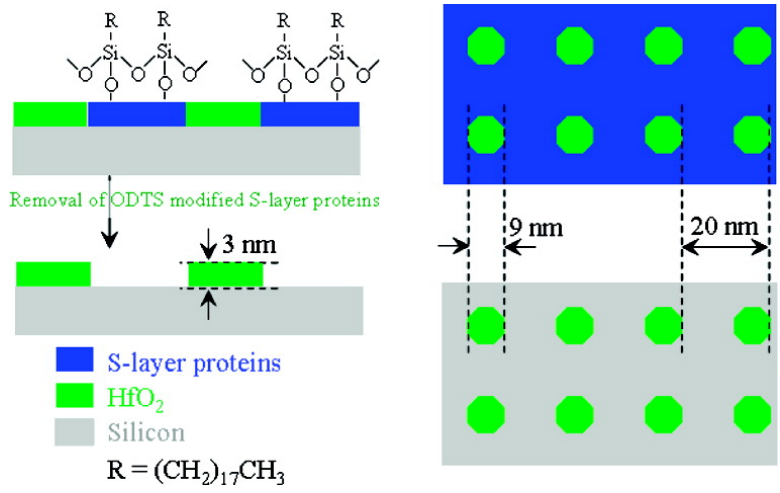

More About This Article

Additional resources and features associated with this article are available within the HTML version:

- Supporting Information
- Access to high resolution figures
- Links to articles and content related to this article
- Copyright permission to reproduce figures and/or text from this article

View the Full Text HTML

J|A|C|S
ARTICLES

Published on Web 11/19/2008

Generation of Oxide Nanopatterns by Combining Self-Assembly of S-Layer Proteins and Area-Selective Atomic Layer Deposition

Jiurong Liu,[†] Yuanbing Mao,[†] Esther Lan,[‡] Diosdado Rey Banatao,[§] G. Jason Forse,[§] Jun Lu,[||] Hans-Olof Blom,[||] Todd O. Yeates,[§] Bruce Dunn,[‡] and Jane P. Chang*[,†]

Departments of Chemical and Biomolecular Engineering, Materials Science and Engineering, and Chemistry and Biochemistry, University of California, Los Angeles, California 90095, and Angstrom Laboratory, Uppsala University, SE-75121 Uppsala, Sweden

Received April 29, 2008; E-mail: jpchang@seas.ucla.edu

Abstract: We report an effective method to fabricate two-dimensional (2D) periodic oxide nanopatterns using S-layer proteins as a template. Specifically, S-layer proteins with a unit cell dimension of 20 nm were reassembled on silicon substrate to form 2D arrays with ordered pores of nearly identical sizes (9 nm). Octadecyltrichlorosilane (ODTS) was utilized to selectively react with the S-layer proteins, but not the Si surface exposed through the pores defined by the proteins. Because of the different surface functional groups on the ODTS-modified S-layer proteins and Si surface, area-selective atomic layer deposition of metal oxide-based high-*k* materials, such as hafnium oxide, in the pores was achieved. The periodic metal oxide nanopatterns were generated on Si substrate after selective removal of the ODTS-modified S-layer proteins. These nanopatterns of high-*k* materials are expected to facilitate further downscaling of logic and memory nanoelectronic devices.

Introduction

Recently, two-dimensional (2D) periodic nanopatterns of functional materials have attracted much attention because of their potential applications in high-density recording media,[1−4] catalysis,[5−8] sensors,[9−12] optoelectronics,[13,14] and electronics.[15−20] In the electronic industry, one of the major driving forces has been its successful downscaling of the dimensions of the metal−oxide semiconductor field effect transistors (MOSFETs). The International Technology Roadmap for Semiconductors 2003 predicted that the device gate length will shrink to 18 nm in 2018.[21] However, device fabrication technologies, such as optical, X-ray, and electron-beam lithography, are limiting factors to produce finer features as the technology node approaches 20 nm considering the diffraction limits of light and also the cost and slow progress of fabricating large areas of periodic nanopatterns.[22] Nanoscale templates, such as the anodic aluminum oxide membranes,[23−28] self-assembled monolayers by polymer nanospheres,[29−32] and block copolymers,[33−45] have been widely investigated to generate nanopatterns, but the feature sizes are usually larger than 20 nm.

S-layer proteins are the outermost component of the cell envelopes of many archaea and bacteria, which are composed

[†] Department of Chemical and Biomolecular Engineering, University of California.
[‡] Department of Materials Science and Engineering, University of California.
[§] Department of Chemistry and Biochemistry, University of California.
[||] Uppsala University.

(1) Sun, S. H.; Murray, C. B.; Weller, D.; Folks, L.; Moser, A. *Science* **2000**, *287*, 1989.
(2) Hehn, M.; Ounadjela, K.; Bucher, J. P.; Rousseaux, F.; Decanini, D.; Bartenlian, B.; Chappert, C. *Science* **1996**, *272*, 1782.
(3) Cheng, J. Y.; Ross, C. A.; Chan, V. Z. H.; Thomas, E. L.; Lammertink, R. G. H.; Vancso, G. J. *Adv. Mater.* **2001**, *13*, 1174.
(4) Fischbein, M. D.; Drndic, M. *Appl. Phys. Lett.* **2005**, *86*, 193106.
(5) Kim, S. W.; Kim, M.; Lee, W. Y.; Hyeon, T. *J. Am. Chem. Soc.* **2002**, *124*, 7642.
(6) Grunes, J.; Zhu, J.; Anderson, E. A.; Somorjai, G. A. *J. Phys. Chem. B* **2002**, *106*, 11463.
(7) Vattuone, L.; Burghaus, U.; Savio, L.; Rocca, M.; Costantini, G.; de Mongeot, F. B.; Boragno, C.; Rusponi, S.; Valbusa, U. *J. Chem. Phys.* **2001**, *115*, 3346.
(8) Adachi, M.; Murata, Y.; Takao, J.; Jiu, J. T.; Sakamoto, M.; Wang, F. M. *J. Am. Chem. Soc.* **2004**, *126*, 14943.
(9) Dong, Y. Z.; Shannon, C. *Anal. Chem.* **2000**, *72*, 2371.
(10) Sirkar, K.; Revzin, A.; Pishko, M. V. *Anal. Chem.* **2000**, *72*, 2930.
(11) Wells, M.; Crooks, R. M. *J. Am. Chem. Soc.* **1996**, *118*, 3988.
(12) Lee, K. B.; Park, S. J.; Mirkin, C. A.; Smith, J. C.; Mrksich, M. *Science* **2002**, *295*, 1702.
(13) Achermann, M.; Petruska, M. A.; Kos, S.; Smith, D. L.; Koleske, D. D.; Klimov, V. I. *Nature* **2004**, *429*, 642.
(14) Peng, C. S.; Huang, Q.; Cheng, W. Q.; Zhou, J. M.; Zhang, Y. H.; Sheng, T. T.; Tung, C. H. *Phys. Rev. B* **1998**, *57*, 8805.
(15) Gudiksen, M. S.; Lauhon, L. J.; Wang, J.; Smith, D. C.; Lieber, C. M. *Nature* **2002**, *415*, 617.
(16) Wallraff, G. M.; Hinsberg, W. D. *Chem. Rev.* **1999**, *99*, 1801.
(17) Maes, H. E.; Claeys, C.; Mertens, R.; Campitelli, A.; Van Hoof, C.; De Boeck, J. *Adv. Eng. Mater.* **2001**, *3*, 781.
(18) Briseno, A. L.; Mannsfeld, S. C. B.; Ling, M. M.; Liu, S. H.; Tseng, R. J.; Reese, C.; Roberts, M. E.; Yang, Y.; Wudl, F.; Bao, Z. N. *Nature* **2006**, *444*, 913.
(19) Yakimov, A. I.; Dvurechenskii, A. V.; Kirienko, V. V.; Yakovlev, Y. I.; Nikiforov, A. I.; Adkins, C. J. *Phys. Rev. B* **2000**, *61*, 10868.
(20) Huang, M. H.; Mao, S.; Feick, H.; Yan, H. Q.; Wu, Y. Y.; Kind, H.; Weber, E.; Russo, R.; Yang, P. D. *Science* **2001**, *292*, 1897.
(21) International Technology Roadmap for Semiconductors; Semiconductor Industry Association: Austin, TX, 2001−2003.
(22) Hulteen, J. C.; Vanduyne, R. P. *J. Vac. Sci. Technol., A* **1995**, *13*, 1553.

10.1021/ja803186e CCC: $40.75

of a single protein or glycoprotein species. S-layer proteins have the intrinsic property to reassemble into 2D arrays on solid support, exhibit different lattice symmetries (p1, p2, p3, p4, and p6) with lattice parameters ranging from 3 to 30 nm, possess a thickness of 5−15 nm, and form periodic nanopores with identical size of 2−8 nm.[46−50] Therefore, the protein architectures have been employed as nanotemplates for fabricating nanostructures.[46,51−57] Using S-layer proteins, for example, researchers have used small cavities as nucleation sites for template-directed synthesis of platinum and palladium nanoparticle arrays.[54] In addition, the S-layer protein of *Deinococcus radiodurans* has been used as an electrodeposition mask to fabricate nanoarrays of metals and metal oxides, including Au, Ni, Pt, Pd, Co, and Cu_2O, over macroscopic substrates.[53] As a result, self-assembling units involving S-layer proteins may be an alternative approach to generate periodic nanopatterns for MOSFETs with feature sizes below 20 nm.

Atomic layer deposition (ALD) refers to the (sub)monolayer deposition of thin films via specific and self-limiting surface reactions.[58] To realize area-selective ALD of metal oxide-based high-*k* material nanopatterns into the nanotemplates composed of protein architectures, it is necessary to modify the S-layer proteins to introduce different surface functional groups upon them and the substrate surface (i.e., silicon substrate) used in this study. As a result, ALD only happens on the Si substrate and cannot take place on the modified surface of the S-layer proteins. Since octadecyltrichlorosilane (ODTS) has been shown to be an effective monolayer resist on a hydrophilic SiO_2 surface toward ALD of HfO_2,[59] in this work, it was chosen to modify the surface of the S-layer proteins but not the Si surface. Specifically, the ODTS-modified S-layer proteins are terminated with aliphatic chains ($R = -(CH_2)_{17}CH_3$), while the Si surface exposed through the pores defined by the protein units is terminated with −OH or −H functional groups. Since atomic layer deposition has been achieved ideally on surfaces with −OH groups and with an incubation time on surfaces with −H groups, it is therefore feasible to achieve area-selective ALD on a surface with a contrast between aliphatic groups and −OH/−H terminations.[59,60] Here, we generated sub-10-nm patterns of high dielectric constant (high-*k*) material on Si substrate, by combining the use of the reassembled S-layer proteins as nanotemplates and an area-selective ALD process.

Experimental Section

S-Layer Protein Preparation. The gene truncation encoding S-layer protein SbsC 258−920 was cloned from purified *Geobacillus stearothermoplilus* genomic DNA into the his-tag (6×) expression vector PET-30 (Stratagene) using the following primers: 5′-GAC GAC GAC AAG ATC CAT ATG GCA GCA TTG ACG CCG AAG G-3′ and 5′-GAG GAG AAG CCC GGT CGG ATC CTT AAG CAT AAT ATA ATT TGT GAC-3′. Successful clones were verified via sequencing and then chemically transformed into the *Escherichia coli* competent cell strain BL21 (DE3) for expressing the functionalized S-layer proteins. One liter of Luria−Bertani broth with 30 mg/L of kanamycin was inoculated from a 5-mL overnight culture and grown shaking at 225 rpm and 37 °C to an OD600 of 0.6. The cells were then induced with 0.4 mM isopropyl-*b*-D-thiogalactopyranoside and grown for an additional 20 h. Cell pellets were collected and frozen at −20 °C. The insoluble and expressed proteins were purified from inclusion bodies using a combination of lysozyme, freeze−thawing, and sonication. Protein pellets were solubilized in 8 M urea and then purified by affinity chromatography using a HisTrap column. Purified his-tag fusion S-layer proteins (his-SbsC 258−920) were dialyzed overnight into 2 M urea. The S-layer proteins were resuspended in a sodium chloride (NaCl) buffer solution (100 mM NaCl and 1.0 mM ethylenediamine tetraacetic acid in 10 mM tris(hydroxymethyl)aminomethane (Tris) hydrochloride, pH 7.0) and stored at 4 °C.

Self-Assembly of S-Layer Proteins. To reassemble the S-layer proteins on the Si wafer, S-layer proteins were first dissolved in

(23) Foss, C. A.; Hornyak, G. L.; Stockert, J. A.; Martin, C. R. *J. Phys. Chem.* **1994**, *98*, 2963.
(24) Martin, C. R. *Science* **1994**, *266*, 1961.
(25) Nielsch, K.; Muller, F.; Li, A. P.; Gosele, U. *Adv. Mater.* **2000**, *12*, 582.
(26) Sander, M. S.; Prieto, A. L.; Gronsky, R.; Sands, T.; Stacy, A. M. *Adv. Mater.* **2002**, *14*, 665.
(27) Zach, M. P.; Ng, K. H.; Penner, R. M. *Science* **2000**, *290*, 2120.
(28) Brumlik, C. J.; Martin, C. R. *J. Am. Chem. Soc.* **1991**, *113*, 3174.
(29) Deckman, H. W.; Dunsmuir, J. H. *Appl. Phys. Lett.* **1982**, *41*, 377.
(30) Kuo, C. W.; Shiu, J. Y.; Cho, Y. H.; Chen, P. *Adv. Mater.* **2003**, *15*, 1065.
(31) Hulteen, J. C.; Treichel, D. A.; Smith, M. T.; Duval, M. L.; Jensen, T. R.; Van Duyne, R. P. *J. Phys. Chem. B* **1999**, *103*, 3854.
(32) Whitney, A. V.; Myers, B. D.; Van Duyne, R. P. *Nano Lett.* **2004**, *4*, 1507.
(33) Thurn-Albrecht, T.; Schotter, J.; Kastle, C. A.; Emley, N.; Shibauchi, T.; Krusin-Elbaum, L.; Guarini, K.; Black, C. T.; Tuominen, M. T.; Russell, T. P. *Science* **2000**, *290*, 2126.
(34) Kim, H. C.; Jia, X. Q.; Stafford, C. M.; Kim, D. H.; McCarthy, T. J.; Tuominen, M.; Hawker, C. J.; Russell, T. P. *Adv. Mater.* **2001**, *13*, 795.
(35) Kim, D. H.; Kim, S. H.; Lavery, K.; Russell, T. P. *Nano Lett.* **2004**, *4*, 1841.
(36) Pai, R. A.; Humayun, R.; Schulberg, M. T.; Sengupta, A.; Sun, J. N.; Watkins, J. J. *Science* **2004**, *303*, 507.
(37) Cha, J. N.; Zhang, Y.; Wong, H. S. P.; Raoux, S.; Rettner, C.; Krupp, L.; Deline, V. *Chem. Mater.* **2007**, *19*, 839.
(38) Qiao, Y. H.; Wang, D.; Buriak, J. M. *Nano Lett.* **2007**, *7*, 464.
(39) Zschech, D.; Kim, D. H.; Milenin, A. P.; Scholz, R.; Hillebrand, R.; Hawker, C. J.; Russell, T. P.; Steinhart, M.; Gosele, U. *Nano Lett.* **2007**, *7*, 1516.
(40) Fisher, A.; Kuemmel, M.; Jarn, M.; Linden, M.; Boissiere, C.; Nicole, L.; Sanchez, C.; Grosso, D. *Small* **2006**, *4*, 569.
(41) Järn, M.; Brieler, F. J.; Kuemmel, M.; Grosso, D.; Lindén, M. *Chem. Mater.* **2008**, *20*, 1476.
(42) Kuemmel, M.; Allouche, J.; Nicole, L.; Boissiere, C.; Laberty, C.; Amenitsch, H.; Sanchez, C.; Grosso, D. *Chem. Mater.* **2007**, *19*, 3717.
(43) Laberty-Robert, C.; Kuemmel, M.; Allouche, J.; Boissiere, C.; Nicole, L.; Grosso, D.; Sanchez, C. *J. Mater. Chem.* **2008**, *18*, 1216.
(44) Park, S.; Kim, B.; Wang, J.-Y.; Russell, T. P. *Adv. Mater.* **2008**, *20*, 681.
(45) Jeong, S.-J.; Xia, G.; Kim, B. H.; Shin, D. O.; Kwon, S.-H.; Kang, S.-W.; Kim, S. O. *Adv. Mater.* **2008**, *20*, 1898.
(46) Sleytr, U. B.; Messner, P.; Pum, D.; Sara, M. *Angew. Chem., Int. Ed.* **1999**, *38*, 1035.
(47) Sleytr, U. B.; Messner P.; Pum D.; Sara, M. In *Crystalline Bacterial Cell Surface Proteins*; Sleytr, U. B., Messner, P., Pum, D., Sara, M., Eds.; Lands Academic Press: Austin, TX, 1996; pp 1−33.
(48) Sleytr, U. B.; Messner, P.; Pum, D. *Methods Microbiol.* **1988**, *20*, 29.
(49) Sleytr, U. B.; Schuster, B.; Pum, D. *IEEE Eng. Med. Biol.* **2003**, *22*, 140.
(50) Toca-Herrera, J. L.; Krastev, R.; Bosio, V.; Kupcu, S.; Pum, D.; Fery, A.; Sara, M.; Sleytr, U. B. *Small* **2005**, *1*, 339.
(51) Shenton, W.; Pum, D.; Sleytr, U. B.; Mann, S. *Nature* **1997**, *389*, 585.
(52) Douglas, K.; Devaud, G.; Clark, N. A. *Science* **1992**, *257*, 642.
(53) Allred, D. B.; Sarikaya, M.; Baneyx, F.; Schwartz, D. T. *Nano Lett.* **2005**, *5*, 609.
(54) Wahl, R.; Mertig, M.; Raff, J.; Selenska-Pobell, S.; Pompe, W. *Adv. Mater.* **2001**, *13*, 736.
(55) Douglas, K.; Clark, N. A.; Rothschild, K. J. *Appl. Phys. Lett.* **1986**, *48*, 676.
(56) Moll, D.; Huber, C.; Schlegel, B.; Pum, D.; Sleytr, U. B.; Sara, M. *Proc. Natl. Acad. Sci. U.S.A.* **2002**, *99*, 14646.
(57) Dieluweit, S.; Pum, D.; Sleytr, U. B. *Supramol. Sci.* **1998**, *5*, 15.
(58) Ritala, M.; Leskela, M. Atomic Layer Deposition. In *Handbook of Thin Film Materials*; Nalwa, H. S., Ed.; Academic Press: London, 2002; Vol. 1, p 103.
(59) Chen, R.; Kim, H.; McIntyre, P. C.; Bent, S. F. *Appl. Phys. Lett.* **2004**, *84*, 4017.
(60) Lao, S. X.; Martin, R. M.; Chang, J. P. *J. Vac. Sci. Technol., A* **2005**, *23*, 488.

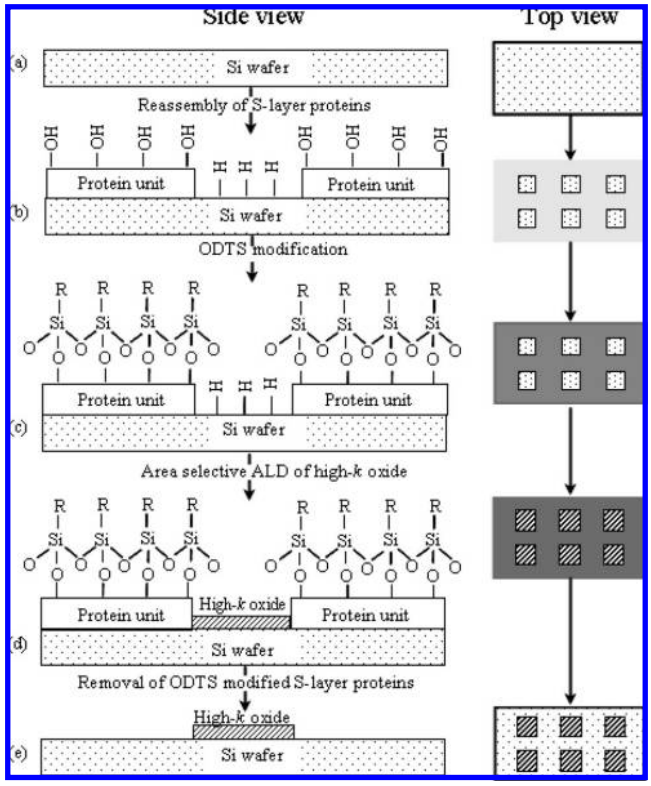

Figure 1. Schematic side view and top view diagrams illustrating the five steps for generating periodic high-*k* oxide nanopatterns on Si substrate by using a nanotemplate of S-layer proteins and an area-selective ALD process.

10× guanidine hydrochloride solution (4 M in 30 mM Tris hydrochloride buffer, pH 8) to disintegrate the assembled proteins into monomers. A 6-mL solution containing the unassembled S-layer proteins was then mixed with 0.6 mL of 100 mM calcium chloride ($CaCl_2$) and centrifuged at 14500 rpm/min for 10 min. The supernatant was then extracted and subsequently diluted as necessary for the reassembling experiments, e.g., by deionized water (10−200×). The experimental procedures are depicted schematically in Figure 1. In step (a), a Si (100) substrate was cleaned by 1 wt % diluted hydrofluoric acid (HF) solution for 15 s to remove the native oxide. In step (b), within two minutes, the HF-cleaned Si substrate was brought into contact with the supernatant containing S-layer proteins and $CaCl_2$ for one hour and subsequently rinsed with deionized water, followed by drying in air.

Surface Modification of Self-Assembled S-Layer Proteins. Following the reassembly of S-layer proteins on the Si surface, in step (c), the sample was immersed into anhydrous toluene solution with 10 mM ODTS for 2−40 h, during which the vials were sealed and held without disturbance. After the ODTS treatment, the sample was subsequently rinsed by toluene, acetone, and chloroform. Step (c) was operated in a dry glovebox purged with N_2.

Area-Selective ALD of HfO_2. In step (d), HfO_2 was deposited from hafnium tetra-*tert*-butoxide (HTB) and H_2O by an ALD process. Each cycle of the ALD process consisted of a 30-s HTB precursor pulse, 90 s of pumping down to a base pressure of 10^{-7} Torr, a 30-s H_2O pulse, followed by another 90 s of pumping to the same base pressure. The substrate temperature was kept at 200 °C during the deposition, and the measured deposition rate was about 1.0 Å/cycle. Finally, in step (e), the sample was annealed in air at 600 °C for 2 h to selectively remove the ODTS-modified S-layer proteins.

Characterization. Following each processing step discussed above, the sample was analyzed by atomic force microscopy (AFM), contact angle measurement, X-ray photoelectron spectroscopy (XPS), and Fourier-transformed infrared spectroscopy (FTIR). Specifically, the S-layer protein nanotemplate and high-*k* oxide nanopattern were examined by a Digital Instruments nanoscope 3A AFM in the tapping mode with a Si tip whose radius is smaller than 10 nm. The contact angle of water was measured with a contact angle analyzer (First Ten Angstroms, FTA 125). The drop images were captured by a video camera after a droplet of deionized water with a volume of 2 μL was suspended on the sample surface and stabilized for at least 5 s. The contact angle was determined as the angle between the substrate surface and a tangent line drawing from the droplet contacting point on the surface. The composition and chemical bonding of the samples were determined by XPS measurements. A Kratos Axis Ultra system with a monochromatic Al Kα source at 1486.8 eV was used to obtain spectra at a takeoff angle of 90° and a pass energy of 20 eV. Shirley background subtraction was performed before the spectral analysis. The compositions were calculated by normalizing the integrated intensity of each element with its atomic sensitivity factor. To complement the XPS analysis, attenuated total reflection FTIR (ATR-FTIR) was performed with a Thermo-Nicolet Nexus 640 infrared spectrometer with a deuterated triglycine sulfate detector in an IR detection range of 250−4000 cm^{-1}. The absorbance spectra were expressed by Beer's law, by taking the ratio of the detector measured intensity of a clean ATR crystal to that of the sample on an ATR crystal.[61] The same processing steps and procedure for cleaning Si wafers were used to carry out the experiments on a Si ATR crystal which is 50-mm long, 10-mm wide, 1-mm thick and has 45° beveled ends. The only exception is the ALD step, since it was not possible to deposit HfO_2 on the Si ATR crystal with the current reactor setup. TEM images were taken with a JEOL JEM-1200EX electron microscope after staining the deposited S-layer protein with uranyl acetate for 3 min. Cross-sectional TEM images were obtained at 300 kV using a FEI Tecnai F30 ST microscope.

Results and Discussion

Si Surface Treatment. To generate a hydrogen-terminated silicon surface, the native SiO_2 layer was removed by HF treatment. The AFM images in Figures 2a and S1a and S2a in the Supporting Information show a root-mean-square (rms) roughness of 3.06 ± 0.16 Å, consistent with literature-reported silicon roughness of 2.6 Å.[62] The contact angle was 64° for the HF-cleaned Si substrate as shown in Figure 3a. There is only a slight change in contact angle from 64 to 61° after the HF-cleaned Si wafer was treated by ODTS in toluene for 2 h (Figure 3a1), suggesting that ODTS does not readily react with Si. On the other hand, the contact angle of the silicon substrate covered with native oxide was measured to be 25°. This value changed to 71° after ODTS treatment for 2 h (results not shown), suggesting that ODTS reacted with the native oxide layer on Si substrate. After HF cleaning, there was a small amount of carbon and oxygen contamination due to the ambient exposure, but there was no oxidation of silicon (no Si−O observed) (Figure 4a).

Self-Assembling S-Layer Proteins on Si Wafer. Figures 2b and S1b and S2b in the Supporting Information show AFM images of S-layer proteins reassembled on an HF-cleaned Si surface. It demonstrated that a 2D array with an identical size of periodic pores, as supported by TEM images (Figure S3a,b in the Supporting Information), was formed on the HF-cleaned Si substrate by the S-layer proteins. From these AFM images, the estimated protein unit cell dimension is about 20 nm, and the pore diameter is about 9 nm. They are in good agreement

(61) Colthup, N. B.; Daly, L. H.; Wiberley, S. E. *Introduction to Infrared and Raman Spectroscopy*, 3rd ed.; Academic Press: San Diego, CA, 1990.
(62) Adachi, S.; Arai, T.; Kobayashi, K. *J. Appl. Phys.* **1996**, *80*, 5422.

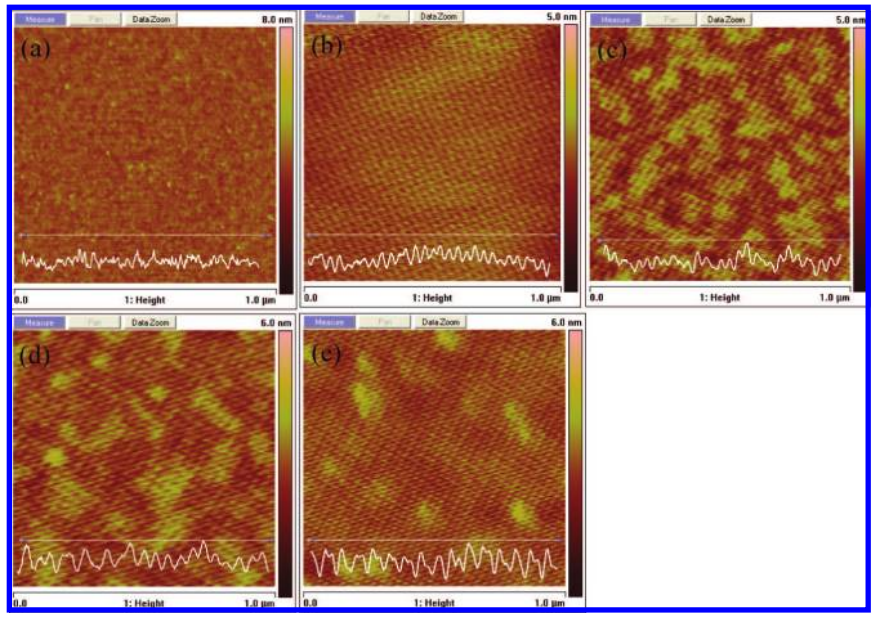

Figure 2. AFM images. (a) HF-cleaned Si substrate. (b) HF-cleaned Si substrate reassembled with S-layer proteins from supernatant with 10 mM $CaCl_2$ for 1 h. (c) Sample (b) subsequently modified by 10 mM ODTS for 2 h. (d) After 30 Å HfO_2 deposited on sample (c). (e) HfO_2 nanopatterns on Si substrate generated by annealing sample (d) in air at 600 °C for 2 h. The line scans in (a)−(e) show the AFM cross section profiles along the lines shown in each image.

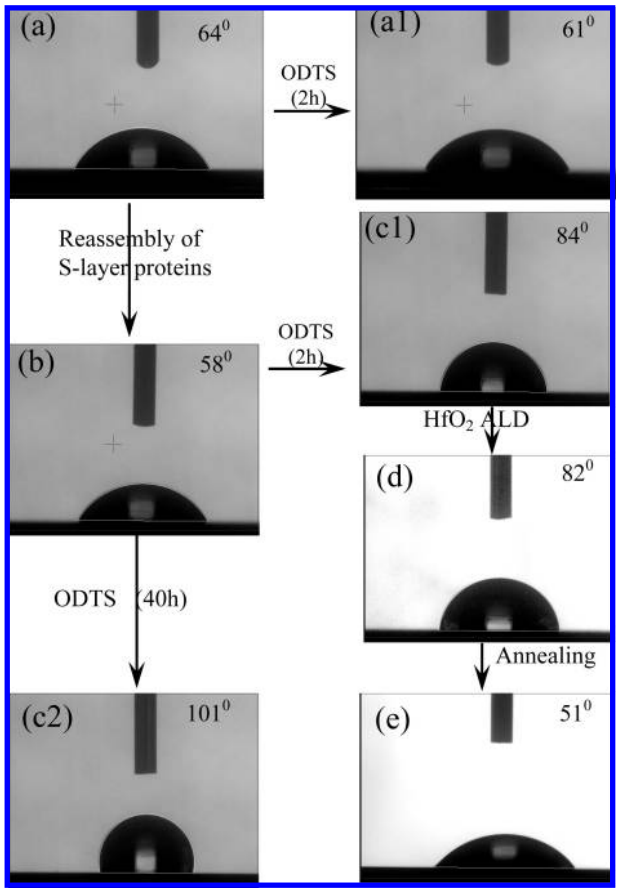

Figure 3. Water contact angle measurements. (a) HF-cleaned Si substrate. (a1) Sample (a) after being modified by 10 mM ODTS in toluene for 2 h. (b) S-layer proteins reassembling on HF-cleaned Si substrate. (c1 and c2) Sample (b) after being modified by 10 mM ODTS in toluene for 2 and 40 h, respectively. (d) Sample (c1) after being deposited with 30 Å HfO_2. (e) Sample (d) after annealing in air at 600 °C for 2 h.

with the values reported in the literature, in which the S-layer proteins showed different lattice symmetries with lattice parameters ranging from 3 to 30 nm and pore sizes varying from 2 to 8 nm.[46−49] The surface rms roughness of reassembled S-layer proteins on Si substrate was 2.73 ± 0.51 Å (Figure 2b), which agreed with the reported roughness of S-layer protein monolayer reassembled on Si substrate ranging from 1.0 to 2.4 Å.[49,63] It suggests an S-layer protein monolayer formed on the HF-cleaned Si substrate. During the protein reassembly, the bivalent cations, Ca^{2+}, act as salt bridge ions and strengthen the interactions among protein units and their attachment to Si surface.[57,63] We found that the surface morphology and roughness strongly depend on the Ca^{2+} cations in the solution. Without the addition of Ca^{2+}, the reassembled S-layer proteins lost the periodicity and islandlike aggregates were observed, while the rms roughness increased to 6.52 Å (Figure S4 in the Supporting Information). The S-layer protein-coated Si surface appeared to be slightly more hydrophilic than the HF-cleaned Si substrate, as the contact angle changed from 64 to 58° (Figure 3b). Unlike the HF-cleaned Si substrate (Figure 5a), the HF-cleaned Si substrate reassembled with S-layer proteins showed the presence of OH (3732 cm^{-1}), NH (3297 cm^{-1}), CH_3 (2968 and 2866 cm^{-1}), CH_2 (2922 cm^{-1}), CO (1645 cm^{-1}), and CN (1525 cm^{-1}), as shown in the IR spectrum (Figure 5b). These vibration modes are known to be the signatures of amino acids,[64,65] which are the building blocks of the S-layer proteins. The XPS analysis confirmed the presence of N, along with a significant increase in the C 1s intensity (Figure 4b). Table 1 summarizes the elemental composition and shows N, C, and O contents to be 12.5, 53.1, and 33.2 atom %, respectively. The combined XPS and AFM analyses (Figures 2b, 4b, and S1b in the Supporting Information), which reveal a very significant concentration of

(63) Gyorvary, E. S.; Stein, O.; Pum, D.; Sleytr, U. B. *J. Microsc. (Oxford, UK)* **2003**, *212*, 300.
(64) Wibowo, S.; Velazquez, G.; Savant, V.; Torres, J. A. *Bioresour. Technol.* **2007**, *98*, 539.
(65) Kazarian, S. G.; Chan, K. L. A. *Biochim. Biophys. Acta* **2006**, *1758*, 858.

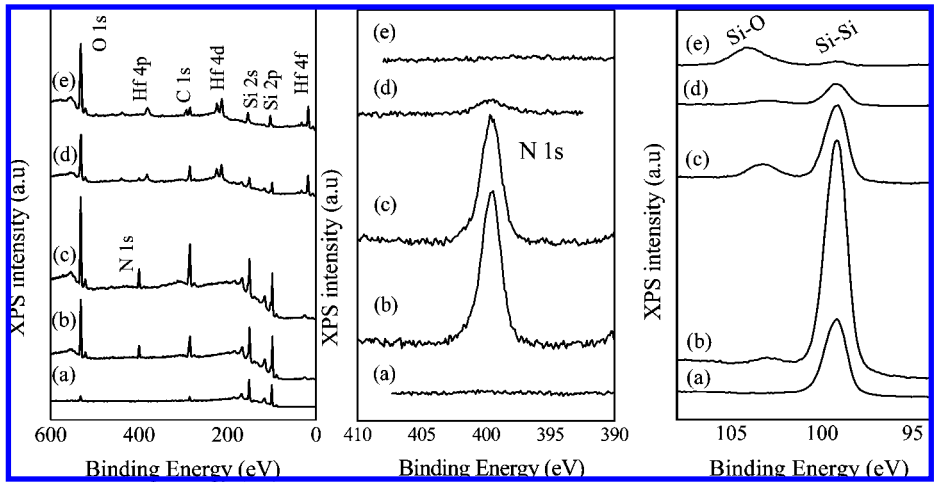

Figure 4. XPS survey scan (left), N 1s (middle), and Si 2p (right) spectra. (a) HF-cleaned Si substrate. (b) HF-cleaned Si substrate with reassembled S-layer proteins on it. (c) Sample (b) after 10 mM ODTS modification for 2 h. (d) Sample (c) after 30 Å HfO_2 deposition. (e) Sample (d) after annealing in air at 600 °C for 2 h.

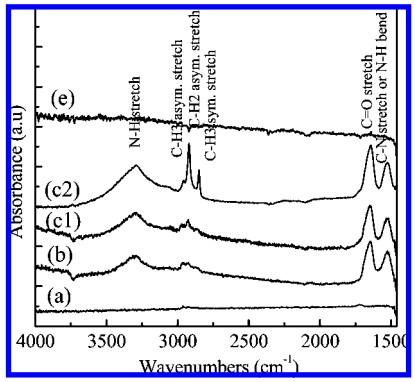

Figure 5. ATR-FTIR spectra. (a) HF-cleaned Si ATR crystal. (b) S-layer proteins reassembled on the HF-cleaned Si ATR crystal. (c1 and c2) Sample (b) after 10 mM ODTS modification for 2 and 40 h, respectively. (e) Sample (c1) after annealing in air at 600 °C for 2 h.

Table 1. N, Hf, C, O, and Si(Si−O) Contents Calculated from XPS Spectra, Corresponding to Samples (a−e) in Figure 2

	element contents atom % (XPS)				
samples	N	Hf	C	O	Si (Si−O)
(a) HF-cleaned Si	0	0	69.3	30.7	0
(b) S-layer reassembled on (a)	12.5	0	53.1	33.2	1.2
(c) ODTS-modified (b)	10.8	0	48.8	34.7	5.7
(d) 30 Å HfO_2 on (c)	5.2	5.2	42.3	42.7	4.6
(e) annealed (d) at 600 °C for 2 h in air	0	4.8	14.8	62.2	18.2

N and periodic surface structure, confirm the reassembly of the S-layer proteins on the Si substrate, as N is the signature element of S-layer proteins. At this point, the Si substrate is slightly oxidized because of the ambient exposure, with approximately 1.2 atom % of Si−O. Compared to the amount of native oxide layer (∼20 Å) normally observed on silicon surface, this suggests that less than 11.3% of the exposed Si surface was oxidized.

ODTS Modification of S-Layer Protein Nanotemplate. Figures 2c and S1c and S2c in the Supporting Information show the AFM images of the ODTS-modified S-layer proteins on Si substrate, with an rms roughness of 4.30 ± 0.33 Å. It is clear that the periodic porous nanopatterns were preserved after the ODTS treatment of the reassembled S-layer proteins. From the AFM images (Figures 2 and S1 and S2b,c in the Supporting Information), the surface morphology showed some variation after the presence of ODTS on the surface, possibly due to the formation of ODTS-containing mounds during the AFM imaging.[66,67] With the ODTS treatment, the contact angle was changed from 58 to 84° after 2 h (Figure 3c1) and to 101° after 40 h (Figure 3c2), due to both the increased roughness of the surface and the higher hydrophobicity of the ODTS-treated S-layer protein surface from the aliphatic chain of the ODTS molecules than the HF-cleaned silicon substrate. The contact angle changes after ODTS treatment on an HF-cleaned and a native oxide-covered Si are from 64 to 61° and from 25 to 71°, respectively. These results suggest that a Si substrate with different surface functionalities after the ODTS modification of reassembled S-layer proteins on HF-cleaned Si substrate is achieved for area-selective ALD. The ATR-FTIR analysis showed that the intensity of the CH_2 absorption peak increased most significantly after ODTS treatment, because of the presence of ODTS molecules composed of 17 CH_2 groups (Figure 5c1,c2). In addition, it was found that the intensity of the CH_2 peak increased with increased exposure to ODTS until a dense monolayer of ODTS molecules was formed on the S-layer protein nanotemplate. The increased intensity of the CH_3 peak after ODTS treatment is due to the terminal CH_3 group from the ODTS molecules. The XPS analysis showed that the C, N, and O contents remained relatively constant (Table 1 and Figure 4c), which indicated that the ODTS treatment did not remove the S-layer nanotemplate from Si substrate. The Si−O component increased from 1.2 to 5.6 atom %, likely due to the formation of covalent Si−O linkages from the reaction of Si−Cl bonds of the ODTS molecules with the hydroxyl groups of S-layer proteins via hydrolyzation reaction, in addition to some further oxidation of Si surface from the ambient exposure. It is known that such a reaction unlikely happens between the Si−Cl bonds of the ODTS molecules and the hydrogen groups of silicon substrate.[68]

(66) De Boer, M. P.; Knapp, J. A.; Michalske, T. A.; Srinivasan, U.; Maboudian, R. *Acta Mater.* **2000**, *48*, 4531.
(67) Lane, J. M. D.; Chandross, M.; Lorenz, C. D.; Stevens, M. J.; Grest, G. S. *Langmuir* **2008**, *24*, 5734.
(68) Hong, J.; Porter, D. W.; Sreenivasan, R.; McIntyre, P. C.; Bent, S. F. *Langmuir* **2007**, *23*, 1160.

Area-Selective ALD of HfO_2. With an ALD process, 30 Å HfO_2 was deposited on the ODTS-modified S-layer protein nanotemplate on Si substrate. The AFM images (Figures 2d and S1d and S2d in the Supporting Information) indicate that a periodic nanostructure was preserved after the HfO_2 deposition with an rms roughness of 4.54 ± 0.16 Å, comparable to that of the ODTS-modified S-layer proteins on Si substrate. This observation indicates that the area-selective ALD has been realized (i.e., HfO_2 is only deposited inside the pores on the Si substrate defined by the S-layer protein units). The measured contact angle is 82° (Figure 3d), which is nearly the same as that of the ODTS-modified S-layer protein monolayer on Si substrate (84°). On the other hand, the contact angle of the Si substrate coated with 30 Å continuous HfO_2 film is 57° (data not shown). The difference in contact angles also confirms the area-selective ALD of HfO_2. The XPS analysis (Table 1 and Figure 4d) showed that the sample contained 5.2 atom % Hf, in addition to 5.2 atom % N and 4.6 atom % Si−O. The Si−O component only showed a little variation from 5.7 to 4.6 atom % after 30 Å HfO_2 deposition, suggesting that the S-layer proteins remained intact without further oxidation of the silicon substrate.

Selective Removal of ODTS-Modified S-Layer Proteins. To remove the ODTS-modified proteins from the HfO_2 nanopatterns on the Si substrate, solution- and gas-phase chemistries were attempted, including the use of a hydrogen peroxide and ammonia solution [1:1:5 = 30% H_2O_2 (aq)/29% NH_4OH (aq)/H_2O] and an energetic oxygen atom beam. Although the reassembled S-layer proteins on Si substrate were completely removed by these methods, none of them were able to selectively remove the S-layer proteins while keeping the HfO_2 nanopattern intact or minimizing the further oxidation of Si substrate. The most effective and simplest method to selectively remove the ODTS-modified S-layer proteins without removal of the HfO_2 nanopattern was by thermal annealing in air at 600 °C for 2 h. All of the organic species were selectively and completely removed by this moderate-temperature thermal annealing procedure, leaving behind the HfO_2 nanopattern. The AFM images (Figures 2e and S1e and S2e in the Supporting Information) and cross-sectional TEM image (Figure S5 in the Supporting Information) confirmed the presence of periodic HfO_2 nanopattern on the Si substrate with feature size of about 9 nm. After annealing, the contact angle decreased to 51° from 82°, which suggests that the S-layer proteins modified with ODTS were removed (Figure 3d,e). As stated earlier, the contact angle of a continuous HfO_2 thin film on Si substrate is 57°, larger than that measured on a native silicon oxide surface (25°). A contact angle of 51° on a HfO_2 nanopattern suggests that it behaves similarly to that of a continuous HfO_2 thin film. The XPS analysis confirmed the complete removal of the S-layer proteins and ODTS molecules from the disappearance of N 1s and a very significant reduction in the C 1s intensity (Table 1 and Figure 4e). The ATR-FTIR analysis (Figure 5e) also confirmed the complete removal of the S-layer proteins and ODTS molecules based on the disappearance of the NH (3297 cm^{-1}), CH_3 (2968 and 2866 cm^{-1}), CH_2 (2922 cm^{-1}), CO (1645 cm^{-1}), and CN (1525 cm^{-1}) vibration modes. The N, C, and H were likely to react with oxygen to form volatile species such as CO, CO_2, H_2O, NO, and NO_2, which resulted in the removal of S-layer proteins and ODTS molecules. Some carbon was still observed, and the amount was consistent with the ambient contamination level. Moreover, Hf 4f intensity remained nearly constant, indicating that the S-layer protein nanotemplate was removed, while HfO_2 did not. The increase of oxidized silicon component (Si−O) from 4.6 to 18.2 atom % was likely due to the oxidation of the exposed Si surface after S-layer proteins were removed at 600 °C in air.

The final obtained periodic nanopatterns of high-*k* oxide with small feature size could facilitate further downscaling of logic and memory nanoelectronic devices. Additionally, the availability of the current nanopatterning method by combining the self-assembly of S-layer proteins with an area-selective ALD technique creates possibilities for fabricating metal and other metal oxide nanopatterns. To further characterize the functionality of this heterogeneous surface, dynamic contact angle measurements are planned in the future. These measurements, combined with the known accessible surface area and the Cassie−Baxter and Cassie−Wenzel models,[69−71] can be used to quantitatively determine the selective functionalization, as recently being demonstrated on a TiO_2/Au system.[41]

Conclusions

S-layer proteins with a unit cell dimension of 20 nm were reassembled on Si substrate to form 2D arrays with periodic pores of nearly identical sizes of 9 nm. ODTS is effective in changing the surface functionality and enabling area-selective ALD. A few-nanometers-thick HfO_2 was deposited by ALD in the pores defined by the S-layer proteins. The periodic HfO_2 nanopatterns with feature size of ~9 nm were achieved on Si substrate after the ODTS-modified S-layer protein nanotemplate was selectively removed by thermal annealing. Therefore, S-layer proteins reassembled on Si substrate acted as a promising nanotemplate for the sub-10-nm nanopatterning of high-*k* oxides for future MOSFET applications.

Acknowledgment. We acknowledge the financial support from the Center on Functional Engineered Nano Architectonics. We thank Carey M. Tanner, Melat Tafesse, and Hyun-Choel (Jeff) Lee for AFM and TEM analyses, and Mark A. Hoffbauer at Los Alamos National Laboratory for testing the stability of S-layer proteins upon reacting with oxygen radicals. We acknowledge the support from the Nanoelectronics Research Facility at UCLA for the AFM analysis and the Chemistry Department at UCLA for the contact angle measurements.

Supporting Information Available: Extra AFM and TEM images. This material is available free of charge via the Internet at http://pubs.acs.org.

JA803186E

(69) Wenzel, R. N. *Ind. Eng. Chem.* **1936**, *28*, 988.
(70) Cassie, A. B. D.; Baxter, S. *Trans. Faraday Soc.* **1944**, *40*, 546.
(71) Cassie, A. B. D. *Discuss. Faraday Soc.* **1948**, *3*, 11.